The Effects of Spatial Configurations of Simulated Shrubs on Wind-proof Effectiveness

Xia Pan[1¶], Zhenyi Wang[1¶], Yong Gao[1, 2*], Zhengcai Zhang[3], Xiaohong Dang [1, 4], Zhongjv Meng [1,4]

[1] *College of Desert Control Science and Engineering, Inner Mongolia Agricultural University, Hohhot, Inner Mongolia Autonomous Region, China*

[2] *Wind Erosion Key Laboratory of Central and Government, Hohhot, Inner Mongolia Autonomous Region, China*

[3] *Key Laboratory of Desert and Desertification, Northwest Institute of Eco-Environment and Resources, Chinese Academy of Sciences, Lanzhou, China*

[4] *National Positioning Observation Research Station of Hangjin Desert Ecosystem, Ordos, Inner Mongolia Autonomous Region, China*

Abstract: Maximizing the benefits of windbreaks requires a thorough understanding of the physical interaction between the wind and the barrier. In this experiment, a profiling set of Pitot tubes was used to measure the airflow field and wind velocity of simulated shrubs in a wind tunnel. The effects of form configurations and row spaces of simulated shrubs on wind-proof effectiveness were in-depth studied. We come to the following results: the weakening intensity of hemisphere-shaped and broom-shaped shrubs on wind velocity was mainly reflected below 2 cm in the root and 6-14 cm in the middle-upper, respectively, while the wind-proof effect of the spindle-shaped shrubs at the canopy (0.2-14 cm height) was the best. Besides, the simulated shrubs under 26.25 cm had the best protection effect on the wind velocity. Moreover, the designed windbreaks with *Nitraria tangutorum*, more effectively reduced the wind velocity among the windbreak compared to behind the windbreak. In the wind control system, the hemisphere-shaped windbreaks should be applied as near-surface barriers, and the windbreaks of broom-shaped and spindle-shaped can be used as a sheltered forest. The results could offer theoretical guidelines on how to arrange the windbreaks for preventing wind erosion in the most convenient and efficient ways.

Keywords: Spatial configuration; Simulated shrubs; Airflow field; Wind velocity; Wind tunnel experiment

1. Introduction

Wind erosion becomes a critical problem and significant threat to land degradation in arid and semiarid regions because it can lower soil productivity, damages plants and constructions, and even causes serious sandstorms (Zhao et al., 2006; Zhang et al., 2017). Wind erosion control aims to reduce surface wind velocity and improve soil resistance (Su et al., 2007; Ma et al., 2010). The most effective management measure to reduce surface wind velocity is to build windbreaks, including natural vegetative shelterbelts and artificial wind barriers (Guan, 2003). However, limited water resources and unique soil texture in arid and semiarid regions can't sustain large vegetative shelterbelt system (Ma et al., 2019). Due to their low cost and water demand, artificial wind barriers have been successfully used in

† The authors contributed equally to this article.
*Correspondence to 13948815709@163.com.

aeolian engineering projects to reduce wind velocity and trap sand grains (Fang, 2018). For example, upright fences made of reed bunches are used in the frontal edge of the shelter system that has been constructed along more than 400 km of highway crossing the shifting dune fields of China's Taklimakan Desert (Dong et al., 2007). Windbreak programs have also been established in Australia (Cleugh et al., 2002), Argentina (Peri and Bloomberg, 2002), South America (Luis and Bloomberg, 2002).

Natural windbreaks may comprise one or more rows of trees while artificial windbreaks are built as thin fences (Li et al., 2018). Windbreaks present a resistance to the approaching airflow, forcing the air to flow at a reduced wind velocity while accelerating it over the top, providing shelter near the ground for some distance leeward of the windbreak. Windbreaks thus slow the airflow and provide shelter for some distance downwind. Wilson and Yee (2003) focused on the reduction of wind velocity near the fences, and the vertical scales were lower than twice the windbreak height. Ma et al., (2019) presented that the inter-row architecture of windbreaks, however, showed a stronger wind reduction inside the windbreak as well as on the lee side than that of the inter-plant architecture. Although many studies have determined the wind-resistant effectiveness of windbreaks, the distribution of airflow field and wind velocity of different kinds of windbreaks is still much debated.

Several measures of the windbreak effectiveness have been agreed that the windbreak effectiveness depends on the shrub's characteristics (canopy shape, density, thickness, and height), on the geometrical arrangement of the trees within the windbreak, and on environmental conditions such as wind velocity and direction, or thermal stratification (Wang et al. 2001). Besides, a review of published results clearly demonstrated that the height, spacing, and height of the spacing ratio of artificial vegetation windbreaks has important influences on the near-surface airflow and on wind erosion. However, for the integrated form configurations of shrubs, the characteristics of the near-surface airflow field and the resulting wind erosion have not been studied. Also, windbreaks have been used for many years to reduce wind velocity as a wind erosion control measure in arid and semiarid regions. However, there is yet no clear answer to what should be the optimal design for windbreaks.

Therefore, we designed a study with the first goal of clarifying the characteristics of the near-surface airflow field above a surface that contains three form configurations and row spaces. Our object was to reveal how to arrange the windbreak forests in terms of form configurations and row spaces for preventing wind erosion in the most convenient and efficient ways. A better understanding of the distribution of the airflow field and wind velocity around the simulated shrubs is essential to optimize windbreak design.

2. Methods

2.1 Setup of the wind tunnel experiment

The wind tunnel used consists of six sections: 1) air inflow, 2) impeller, 3) flow stabilization, 4) flow contraction, 5) test section, and 6) outflow diffusion section. The wind tunnel is 37.78 m long with a test section of 16.23 m (Length) ×0.6 m (Height) ×1 m (Width) (Figure 1). The wind velocity within the wind tunnel was continuously adjustable from 1 m/s to 40 m/s (turbulence intensity < 0.4%), with a measurement precision of ± 2% to ± 0.5%. The thickness of the boundary layer in the test section is typically more than 120 mm. Inside the test section, 3 cm thick unpolished wooden boards were used to cover the whole test

section floor to simulate the rough ground in the field and were also used as bases to fix the simulated shrubs.

2.2 Structure and characteristic of simulated shrubs with different form configurations

Before the wind tunnel experiments, we measured the characteristics of annual *Nitraria tangutorum* in the field, including height, canopy dimension, and canopy porosity (Table 1). The canopy dimensions were measured by the long diameter × width diameter × thickness of the leaf. The optical porosity of the plants' canopies was estimated by using an unsupervised classification analysis of canopy photographs using the software ERDAS IMAGINE 9.2 (https://www.hexagongeospatial.com) (Ma et al., 2019). Accordingly, the simulated shrubs used in this study were at a scale of 1:4 according to the geometric morphology and canopy porosity of field plants.

Simulated shrubs were constructed from a new type of wind-resistant material that is polymerized by anti-aging polymer compounds. Their leaves simulate those of *Nitraria tangutorum*. Compared with the traditional materials of windbreaks, the life of the simulated shrubs is more than 15 years. The overall heights of simulated shrubs were 22 cm, of which the ground height was 17.5 cm and the underground length was 4.5 cm. The number of main branches was 8-10 and each main branch contained 10-15 leaves. The simulated shrubs lacked the main trunk. To enable the stimulated shrubs to stand upright, the branches were constructed of iron wires wrapped in plastic. Based on the features of branches and leaves of *Nitraria tangutorum* in the field, three form configurations of spindle-shaped, broom-shaped, and hemisphere-shaped were customized. Each row included five shrubs evenly placed on the foam board. And we kept the porosity, canopy shape, density, thickness, and height for each form configuration as the same. A schematic diagram of the spatial configurations is shown in Figure 2.

2.3 Measurements of wind velocity

Wind velocity of 8, 12, and 16 m/s at different heights were measured using a profiling set of Pitot tubes along the central axis of the wind tunnel, namely 0.2, 0.5, 1, 2, 4, 8, 12, 16, 20, and 24 cm. Measurement of wind velocities began from 0.5H (8.75 cm in front of the first row of simulated shrubs) windward of the first row to M0.5H (between the first and second rows of simulated shrubs), M1.5H (between the second and third rows of simulated shrubs) the middle among the three rows and to B0.5H (8.75 cm in behind of the third row of simulated shrubs), B1H (17.5 cm in behind of the third row of simulated shrubs), B3H (52.5 cm in behind of the third row of simulated shrubs), B5H (87.5 cm in behind of the third row of simulated shrubs) leeward of the last row (H is 17.5 cm which is the ground height of the stimulated shrubs). At each measurement point, the wind velocities were measured for 60 s and the resolution of Pitot tubes is 1 s. The row spaces were 17.5 cm, 26.25 cm, and 35 cm, respectively. Finally, wind velocity was determined by the wind pressure signals continuously using a micro-differential-pressure sensor with FSKX-10.

It is noted that we calculated the Reynolds number (Re) using the equation by Wu and Yang (2013) as a criterion to determine the dynamic similarity in the wind-tunnel measurement, the calculated Re is 6.9×10^4 - 12×10^4. Thus, this means that a fully turbulent

flow environment and self-similarity requirement for the wind tunnel simulation was achieved (Qu et al., 2001; Wu and Yang, 2013).

2.4 Data analysis

Contour maps were made based on the Kriging interpolation algorithm by using version 14.0 of the Surfer software (https://www.goldensoftware.com/). Other graphs were made in version 8.0 of the OriginPro software (https://www.originlab.com/).

3. Results and analysis

3.1 The airflow field of different form configurations and row spaces

The airflow field of wind velocity represents the distribution characteristics of transit wind velocity in specific areas. The contour of wind velocity presented the magnitude and change of wind velocity. Figure 3-5 showed that the darker the color, the smaller the wind velocity; the denser the contour line, the greater the change in wind velocity. According to the contour value of wind velocity in this study, it can be found that the zone with wind velocity <9.8 m/s is the deceleration zone with the dark area, however, the zone with wind velocity >9.8 m/s is the acceleration zone with the light area.

The airflow field of different spatial configurations with simulated shrubs (A, B, C represents hemisphere-shaped, spindle-shaped, and broom-shaped, respectively) under different net wind velocities (8 m/s, 12 m/s, and 16 m/s) in 17.5 cm is shown in Figure 3. The airflow field characteristics of simulated shrubs with different spatial configurations were different. The weakening zone of wind velocity in hemisphere-shaped simulated shrubs was mainly concentrated below 2 cm in the root and 7-13 cm in the middle-upper, and the weakening degree of wind velocity in the root was stronger than that in the middle-upper. And the contour of the root was denser, which indicated that the wind velocity changed greatly here. The airflow field of hemisphere-shaped shrubs at 16 m/s showed a concentrated continuous distribution, while the distribution of airflow field at 8 m/s and 12 m/s was similar. The reduced strength of spindle-shaped simulation shrubs to wind velocity was better than that of hemisphere-shaped and broom-shaped. The weakening height of the wind velocity of the spindle-shaped simulated shrubs under different net wind velocities was mainly concentrated below 14 cm. Besides, the contour at 16 m/s was denser, indicating that the variation of wind velocity was large. Spindle-shaped simulated shrubs had a more uniform weakening range of wind velocity, and the protective effect was better. The reduction height of wind velocity was mainly concentrated at 6-14 cm in the middle-upper. The decrease of wind velocity near the root was small, and it showed a weakening trend with the increase of net wind velocities. Besides, the reduction in wind velocity in the broom-shaped simulated shrubs began after the first row of simulated shrubs. Broom-shaped simulated shrubs under 16 m/s were less effective at protecting against wind velocity.

Figure 4 is the airflow field of different spatial configurations with simulated shrubs (A, B, C represents hemisphere-shaped, spindle-shaped, and broom-shaped, respectively) under different net wind velocities (8 m/s, 12 m/s, and 16 m/s) in 26.25 cm. Compared with 17.5 cm, the reduced intensity and range of wind velocity were significantly increased in different simulation shrubs with spatial configurations under 26.25 cm. The reduction of wind velocity in the hemisphere-shaped and broom-shaped simulated shrubs was mainly reflected in the

two zones, which were below 4cm in the root, and 6-14 cm in the middle and upper, respectively. And the reduction intensity of wind velocity decreased at 16 m/s, but the changing trend of wind velocity was more stable. The spindle-shaped simulation shrubs had a strong weakening degree of wind velocity, and the weakening range was more uniform. Besides, the weakening height of spindle-shaped simulation shrubs was mainly below 14 cm. The airflow field of different spatial configurations with simulated shrubs (A, B, C represents hemisphere-shaped, spindle-shaped, and broom-shaped, respectively) under different net wind velocities (8 m/s, 12 m/s, and 16 m/s) in 35 cm is shown in Figure 5. The weakening height of the wind velocity of the hemisphere-shaped simulated shrub was mainly concentrated below the root 2 cm, and the weakening degree of the wind velocity in the middle and upper part was relatively weak. With the increase of net wind velocity, the protective effect of hemisphere-shaped simulated shrubs on wind velocity gradually decreased. The reduced height of the spindle-shaped simulated shrubs for wind velocity was mainly reflected below 14 cm, and the weakening range was more uniform. The contour of the spindle-shaped simulated shrubs at 16 m/s was denser, indicating that the wind velocity fluctuated greatly at this time. The reduction height of wind velocity of the broom-shaped simulated shrubs was mainly concentrated below 2 cm in the root and 6-14 cm in the middle and upper. And the variations of wind velocity at 8 m/s and 12 m/s were more unstable than at 16 m/s.

3.2 The average wind velocity of Pitot tubes in different measurement heights

Figure 6 is the distribution of average wind velocity of Pitot tubes in different heights of different spatial configurations with simulated shrubs (hemisphere-shaped, spindle-shaped, and broom-shaped), row spaces (17.5 cm, 26.25 cm, and 35 cm), and net wind velocities (8 m/s, 12 m/s, and 16 m/s). The reduction of wind velocity by simulated shrubs with the different spatial configurations was mainly concentrated between 0.2-12 cm, and the wind velocity above 16 cm was larger, which indicated that the simulated shrubs had an obvious effect on reducing wind velocity. These results are consistent with the distribution of airflow fields of different spatial configurations with simulated shrubs. Simulated shrubs at 0.5 cm under different net wind velocities had the strongest effect on the reduction of wind velocity. With the increase of row space at the same net wind velocity, the variation of simulated shrubs with the different spatial configurations was similar, which indicated that the influence of row space on the average wind velocity of Pitot tubes in different heights was relatively slight. Compared with other simulated shrubs with different spatial configurations, the wind velocity of the broom-shaped simulated shrubs below 16 cm was weakened more strongly.

3.3 The average wind velocity at the canopy and above the canopy

Profile of average wind velocity of different spatial configurations with simulated shrubs (hemisphere-shaped, spindle-shaped, and broom-shaped), row spaces (17.5 cm, 26.25 cm, and 35 cm), and net wind velocities (8 m/s, 12 m/s, and 16 m/s) is shown in Figure 7. The net wind velocity at the canopy is the average value of 0.2 cm, 0.5 cm, 1 cm, 2 cm, 4 cm, 8 cm, 12 cm, 16 cm, and the net wind velocity above the canopy is the average value of 20 cm and 24 cm. The average wind velocity above the canopy of simulated shrubs with different spatial configurations under net wind velocities was higher than at the canopy. And the average wind

velocity increased with the improvement of net wind velocity. Although the overall patterns of wind velocity were similar, it is noteworthy that an acceleration zone of wind velocity above the canopy was observed in M0.5H to B0.5H because the average wind velocity above the canopy presented firstly increased and then decreased. However, the average wind velocity at the canopy showed the opposite trend. Therefore, the wind-proof effect at the canopy (0.2-16 cm height) was the best.

3.4 The average wind velocity at different measuring distances

Average wind velocity of different spatial configurations with simulated shrubs (hemisphere-shaped, spindle-shaped, and broom-shaped), row spaces (17.5 cm, 26.25 cm, and 35 cm), and net wind velocities (8 m/s, 12 m/s, and 16 m/s) is shown in Figure 8. Broom-shaped simulated shrubs in the front row (0.5H) in 17.5 cm had a better reduction strength to wind velocity than hemisphere-shaped and spindle-shaped but the wind-proof effect of spindle-shaped simulated shrubs between the first row and the second row (M0.5H) was optimal. The simulated shrubs of different distances in 17.5 cm had different weakening degrees of wind velocity and a large variation. With the increase of row space and net wind velocity, the weakening effect of broom-shaped simulated shrubs on wind velocity was gradually enhanced and stable, especially the wind-proof effect of broom-shaped simulated shrubs in 35 cm was better than spindle-shaped and hemisphere-shaped. Therefore, the wind velocity of the simulated shrubs in 35 cm was relatively stable, and the wind-proof effect of spindle-shaped simulated shrubs was the best. Besides, with the increase of the distance, the effect of the simulated shrubs on the wind velocity was first decreasing and then rising slowly. The weakening effect of simulated shrubs with different spatial configurations from M0.5H to B0.5H on wind velocity was better than that of B1H to B5H.

4. Discussion

In aeolian engineering projects, it is normal for windbreaks to built-in a suitable inter-row space to improve the roughness of soil surface and reduce the average wind velocity (Ma et al., 2010; Li et al., 2018). The optimal inter-row space can promise the best shelter effect required at a minimal cost (Fang et al., 2018). By using the Computational Fluid Dynamics (CFD) method, Fang et al. (2018) recommended the double-row windbreaks with inter-row space of 6H is the best design for windbreaks. Lima et al. (2017) concluded by using numerical simulations that an array fence needs at least 4 rows and an equal interval. However, in this study, the simulated shrubs of row space under 26.25 cm had the best protection effect on the wind velocity (Figure 4). And average wind velocity of different measuring distances presented that the weakening effect of simulated shrubs with different spatial configurations from M0.5H to B0.5H on wind velocity was better than that of B1H to B5H (Figure 8). And other studies also showed that the inter-row architecture of windbreaks showed a stronger reduction of wind velocity at a given distance, suggesting more effective surface protection when this type of windbreak is used to reduce wind erosion (Wu et al., 2015; Li et al., 2018). It might be expected that there was a cumulative effect that would cause larger wind reductions behind second and successive windbreaks than behind the first in a series of parallel windbreaks (Cui and Neary, 2008).

Moreover, we found that the designed windbreak with *Nitraria tangutorum*, more effectively reduced the wind velocity among the windbreak compared to behind the windbreak (Figure 8). Mirhasani et al. (2019) showed that the wind velocity behind the second row of the windbreaks decreased significantly, and it is more obvious that the wind velocity accelerated rapidly and approached the initial wind velocity from the 80 m behind the first row, which is the same from ours. Jia et al. (2019) reported that when the row space was smaller than 5H, the wind velocity between adjacent rows in the near-surface layer changed slightly. And the results of this study are also in agreement with the results of Cook and Goyens (2008), and Refahi (2012). Besides, in this study, the wind velocity at the canopy (0.2-14 cm height) was extremely low, and where the wind velocity was generally higher in the upper layers (>14 cm) (Figure 3-5). The wind profiles demonstrated the potential blocking effect of the simulated shrubs which was responsible for wind velocity reduction at the height of the simulated shrubs (0.2-14 cm), where the effect of the simulated shrubs area on wind velocity was enhanced. Researches presented the reason for wind velocity increasing above the simulated shrubs is the development of strong turbulence and shear stress (Finnigan, 2000; Dupont and Brunet, 2008; Dupont et al., 2011).

Considering that the weakening intensity of hemisphere-shaped and broom-shaped shrubs on wind velocity was mainly reflected below 2 cm in the root and 6-14 cm in the middle and upper, respectively, while the wind-proof effect of the spindle-shaped simulated shrubs at the canopy (0.2-14 cm height) was the best (Figure 3-5). So three kinds of windbreaks can be used in a combination in a wind control system. The hemisphere-shaped windbreaks should be applied as near-surface barriers, and windbreaks of broom-shaped and spindle-shaped can be used as a sheltered forest. The system not only can integrate wind control but also can benefit the landscape beautification vision in desert areas. Although the optimal design of windbreak depends strongly on the purpose for which it is constructed, such as the protection of a field from wind erosion or the protection of infrastructure from being destroyed (Cornelis and Gabriels, 2005), it is also necessary to understand the general abilities of windbreaks in reducing wind velocity. Therefore, these analytical findings will likely prove useful in terms of designing ecological habitats and preventing wind erosion in arid and semiarid desert areas.

Besides, windbreak density, porosity distribution, height, orientation, and width all also influence wind velocity reduction and turbulence intensity in the lee of windbreaks. Free wind velocity and the surface roughness of the surrounding area also affect windbreak performance (Cornelis and Gabriels, 2005; Van et al., 2014). We will further conduct study in these aspects to give more practical optimized windbreak design to provide a more insightful reference for aeolian engineering.

5. Conclusion

Based on the observed airflow fields and wind profiles above the surface that contained ridges, we concluded that the weakening intensity of hemisphere-shaped and broom-shaped shrubs on wind velocity was mainly reflected below 2 cm in the root and 6-14 cm in the middle and upper, respectively, while the wind-proof effect of the spindle-shaped simulated

shrubs at the canopy (0.2-14 cm height) was the best. Besides, with the increase of distance, the weakening effect of each form configuration of simulated shrubs on wind velocity showed the trend of first decreasing and then slowly increasing, and the weakening effect at M0.5H-B0.5H was better than that of B1H-B5H. From the weakening intensity and range of the wind velocity, the simulated shrubs under 26.25 cm had the best protection effect on the wind velocity. Moreover, the designed windbreak with *Nitraria tangutorum*, more effectively reduced the wind velocity among the windbreak compared to behind the windbreak. In the wind control system, the hemisphere-shaped windbreaks should be applied as near-surface barriers, and the windbreaks of broom-shaped and spindle-shaped can be used as a sheltered forest.

Acknowledgments

We acknowledge the Key Laboratory of Desert and Desertification of the Chinese Academy of Sciences for using the wind tunnel.

Funding

This research was financially supported by the National Natural Science Foundation of China [41967009] and the China Scholarship Council [201908150155].

Declaration of competing interests

The authors declared no potential conflicts of interest with respect to the research, authorship, and/or publication of this article.

References

Cleugh, H.A., R. Prinsley, R.P. Bird, S.J. Brooks, P.S. Carberry, M.C. Crawford, T.T. Jackson, J. Minke, S.J. Mylius, I.K. Nuberg, R.A. Sudmeyer, and A.J. Wright. 2002. The Australian National Windbreaks Program: Overview and summary of results. Aust. J. Exp. Agric. 42:649-664.

Cui, J., Neary, V.S., 2008. LES study of turbulent flows with submerged vegetation. J. Hydraul. Res. 46(3), 307-316.

Cook, G. D., Goyens, C. M., 2008. The impact of wind on trees in Australian tropical savannas: lessons from Cyclone Monica. Austral Ecology, 33, 462-470.

Cornelis,W.M, Gabriels, D., 2005. Optimal windbreak design for wind-erosion control. Journal of Arid Environments, 61(2), 315-332.

Dong, Z.B., Luo, W., Qian, G.Q., Wang, H.T., 2007. A wind tunnel simulation of the mean velocity fields behind upright porous fences. Agricultural and Forest Meteorology, 146, 82-93.

Dupont, S., Brunet, Y., 2008. Edge flow and canopy structure: a large-eddy simulation study. Bound.-Layer Meteorology, 126, 51-71.

Dupont, S., Bonnefond, J.-M., Irvine, M.R., Lamaud, E., Brunet, Y., 2011. Long-distance edge effects in a pine forest with a deep and sparse trunk space: in situ and numerical experiments. Agricultural Meteorology, 151, 328-344.

Fang, H., Wu, X.X., Zou, X.Y., Yang, X.F., 2018. An integrated simulation-assessment study for optimizing wind barrier design. Agricultural and Forest Meteorology, 263, 198-206.

Finnigan, J., 2000. Turbulence in plant canopies. Annual Review of Fluid Mechanics, 32, 519-571.

Guan, D., Zhang, Y., Zhu, T., 2003. A wind-tunnel study of windbreak drag. Agricultural and Forest Meteorology, 118, 75-84.

Jia, W.R., Zhang, C.L., Zou, X.Y., Cheng, H., Kang, L.Q., Liu, B., Li, J.F., Shen, Y.P., Liu, W., Fang, Y., Li, H.R., 2019. Effects of ridge height and spacing on the near-surface airflow field and on wind erosion of a sandy soil: Results of a wind tunnel study, Soil and Tillage Research, 186, 94-104.

Luis, P.P., Bloomberg, M., 2002. Windbreaks in southern Patagonia, Argentina: A review of research on growth models, wind speed reduction, and effects on crops, Agroforestry System, 56, 129-144.

Li, X., Ma, Y., Ma, R., Zhang, Y., Tang, W., Yang, J., 2018. Wind flow field and windproof efficiency of shelterbelt in different width. J. Desert Res. 38(5), 936-944.

Lima, I.A., Araújo, A.D., Parteli, E.J.R., Andrade, J.S., Herrmann, H.J., 2017. Optimal array of sand fences. Sci. Rep. 7, 45148.

Ma, R., Wang, J., Qu, J., Liu, H., 2010. Effectiveness of shelterbelt with a non-uniform density distribution. J. Wind Eng. Ind. Aerodyn. 98(12), 767-771.

Ma, R., Li, J.R., Ma, Y.J., Shan, L.S., Li, X.L., Wei, L.Y., 2019. A wind tunnel study of the airflow field and shelter efficiency of mixed windbreaks. Aeolian Research, 41, 1875-9637.

Mirhasani, M., Rostami, N., Bazgir, M., Tavakoli, M., 2019. Living windbreak design for wind erosion control in arid regions: A case study in Dehloran, Iran. Desert, 24, 33-42.

Peri, P.L., and M. Bloomberg. 2002. Windbreaks in southern Patagonia, Argentina: A review of research on growth models, wind speed reduction, and eff ects on crops. Agrofor. Syst. 56, 129-144.

Qu, J.J., Liu, X.W., Lei, J.Q., Li, F., Yu, Z.Y., 2001. Simulation experiments on sand arresting effect of nylon net fence in wind tunnel. J. Desert Res. 21, 276-280 (in Chinese).

Refahi, H. Gh., 2012. Wind Erosion and conservation, Tehran University Press, 6th Edition, 320 P.

Su, Y.Z., Zhao, W.Z., Su, P.X., Zhang, Z.H., Wang, T., Ram, R., 2007. Ecological effects of desertification control and desertified land reclamation in an oasis-desert ecotone in an arid region: a case study in Hexi Corridor, northwest China. Ecol. Eng. 29(2), 117-124.

Van, T.D., Van, Do.T., Sato, T., Huang, T.T., 2014. Effects of species and shelterbelt structure on wind speed reduction in shelter. Agroforestry Systems, 88, 237-244.

Wilson, J.D., Yee, E., 2003. Calculation of winds disturbed by an array of fences, Agricultural Meteorology, 115, 31-50.

Wang, H., Takle, E.S, Shen, J., 2001. Shelterbelts and windbreaks: mathematical modeling and computer simulations of turbulent flows. Annual Review of Fluid Mechanics, 33, 549-586.

Wu, B., Yang, H., 2013. Spatial patterns and natural recruitment of native shrubs in a semi-arid sandy land. PLOS ONE, 8(3), e58331.

Wu, X., Zou, X., Zhou, N., Zhang, C., Shi, S., 2015. Deceleration efficiencies of shrub windbreaks in a wind tunnel. Aeolian Res. 16, 11-23.

Zhao, H. L., Zhou, R.L., Zhao, X.Y., Zhang, T.H., Drake, S. 2006. Wind erosion and sand accumulation efects on soil properties in Horqin Sandy Farmland, Inner Mongolia. Catena, 65(1), 70-79.

Zhang, Z.C., Dong, Z.B., Qian, G.Q., 2017. Field observations of the vertical distribution of sand transport characteristics over fine, medium and coarse sand surfaces, 42(6), 889-902.

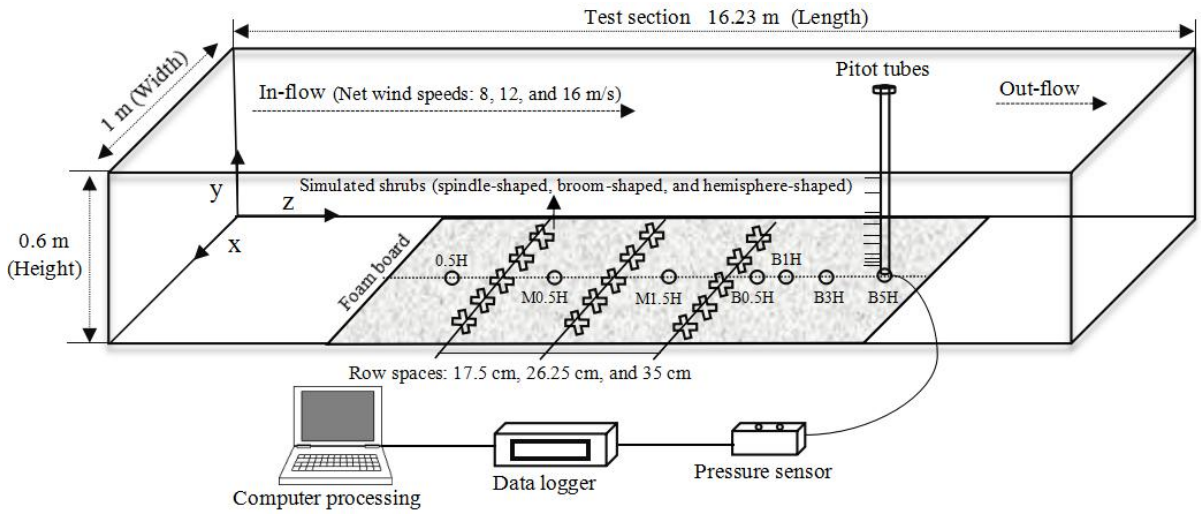

366 Figure 1 Test section of wind tunnel

367

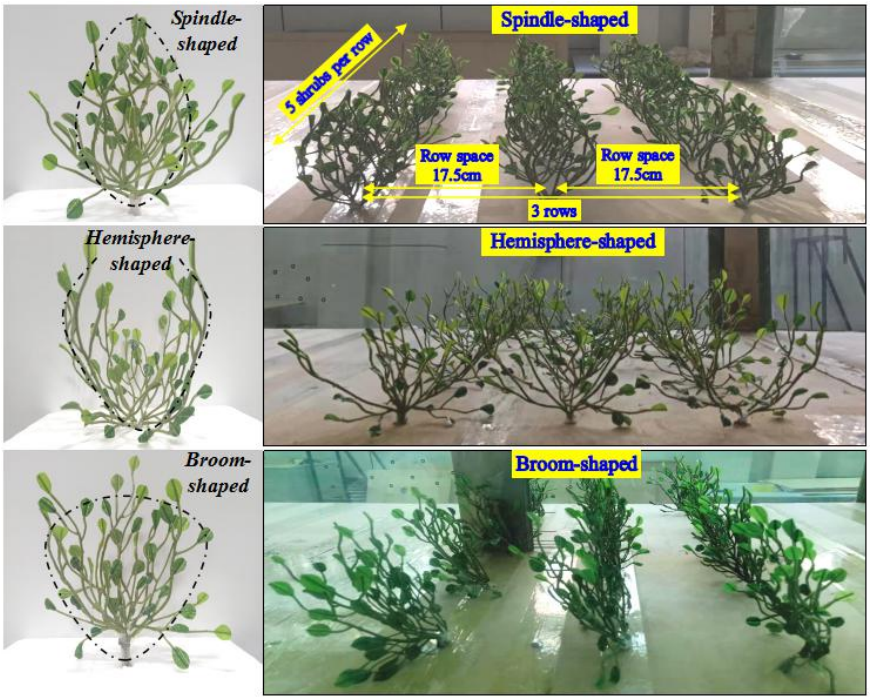

368 Figure 2 Spatial configurations of simulated shrubs (left) and a schematic diagram of the wind tunnel laboratory
369 (right)

370

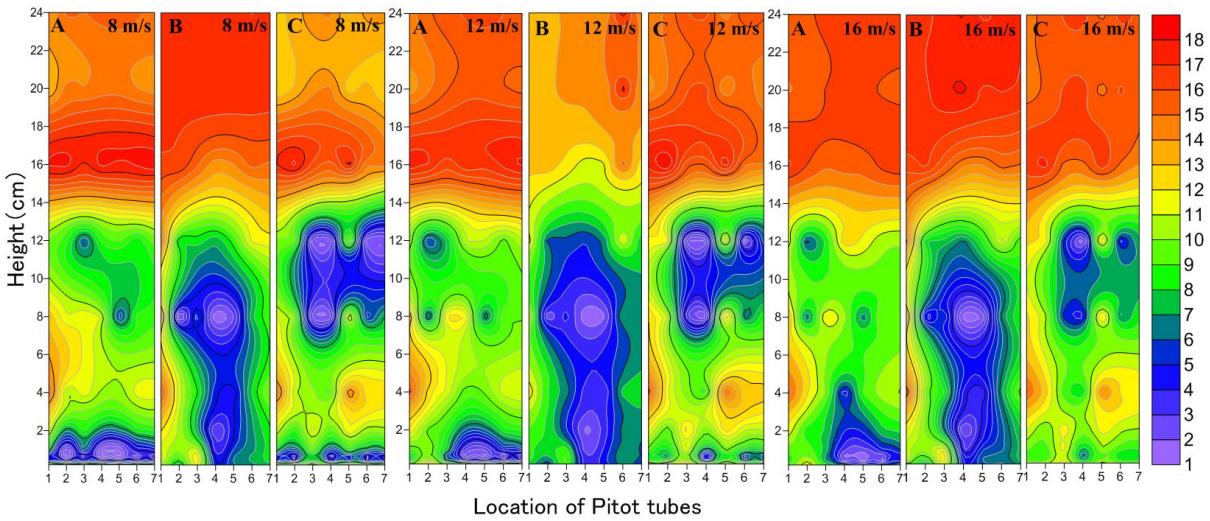

371 Figure 3 The airflow field of different spatial configurations with simulated shrubs (A, B, C represents
372 hemisphere-shaped, spindle-shaped, and broom-shaped, respectively) under different net wind velocities (8 m/s,
373 12 m/s, and 16 m/s) in 17.5 cm (Horizontal axis 1-7 corresponds to 0.5H, M0.5H, M1.5H, B0.5H, B1H, B3H,
374 and B5H, respectively)

375

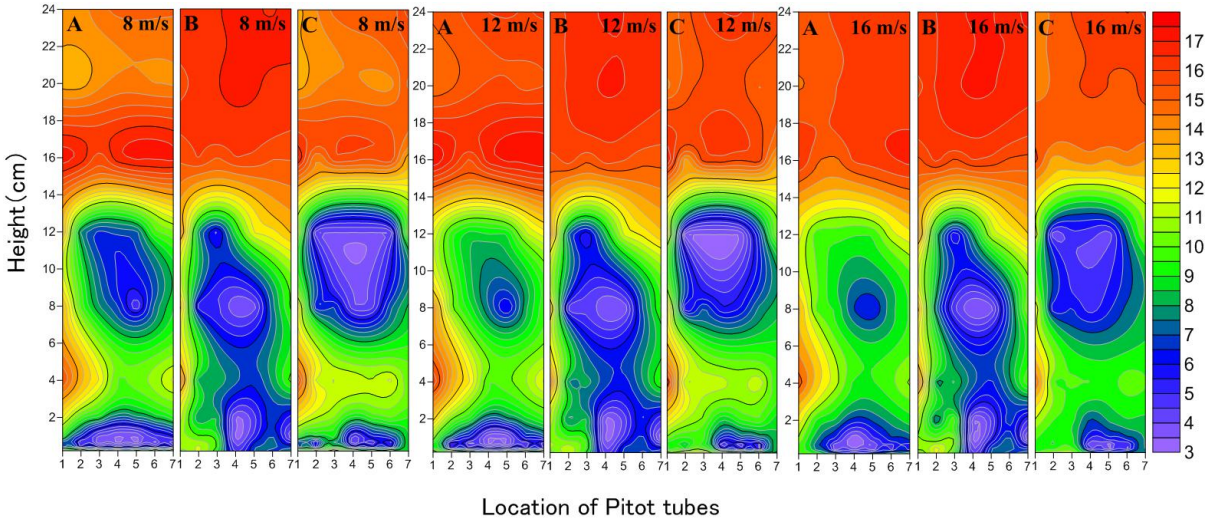

376 Figure 4 The airflow field of different spatial configurations with simulated shrubs (A, B, C represents
377 hemisphere-shaped, spindle-shaped, and broom-shaped, respectively) under different net wind velocities (8 m/s,
378 12 m/s, and 16 m/s) in 26.25 cm (Horizontal axis 1-7 corresponds to 0.5H, M0.5H, M1.5H, B0.5H, B1H, B3H,
379 and B5H, respectively)

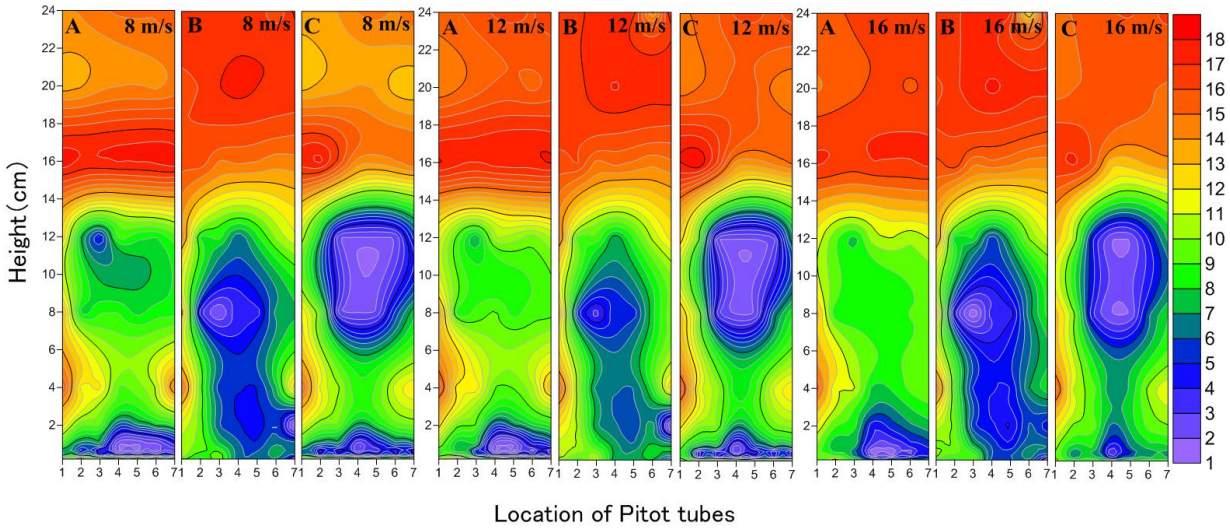

Figure 5 The airflow field of different spatial configurations with simulated shrubs (A, B, C represents hemisphere-shaped, spindle-shaped, and broom-shaped, respectively) under different net wind velocities (8 m/s, 12 m/s, and 16 m/s) in 35 cm (Horizontal axis 1-7 corresponds to 0.5H, M0.5H, M1.5H, B0.5H, B1H, B3H, and B5H, respectively)

385

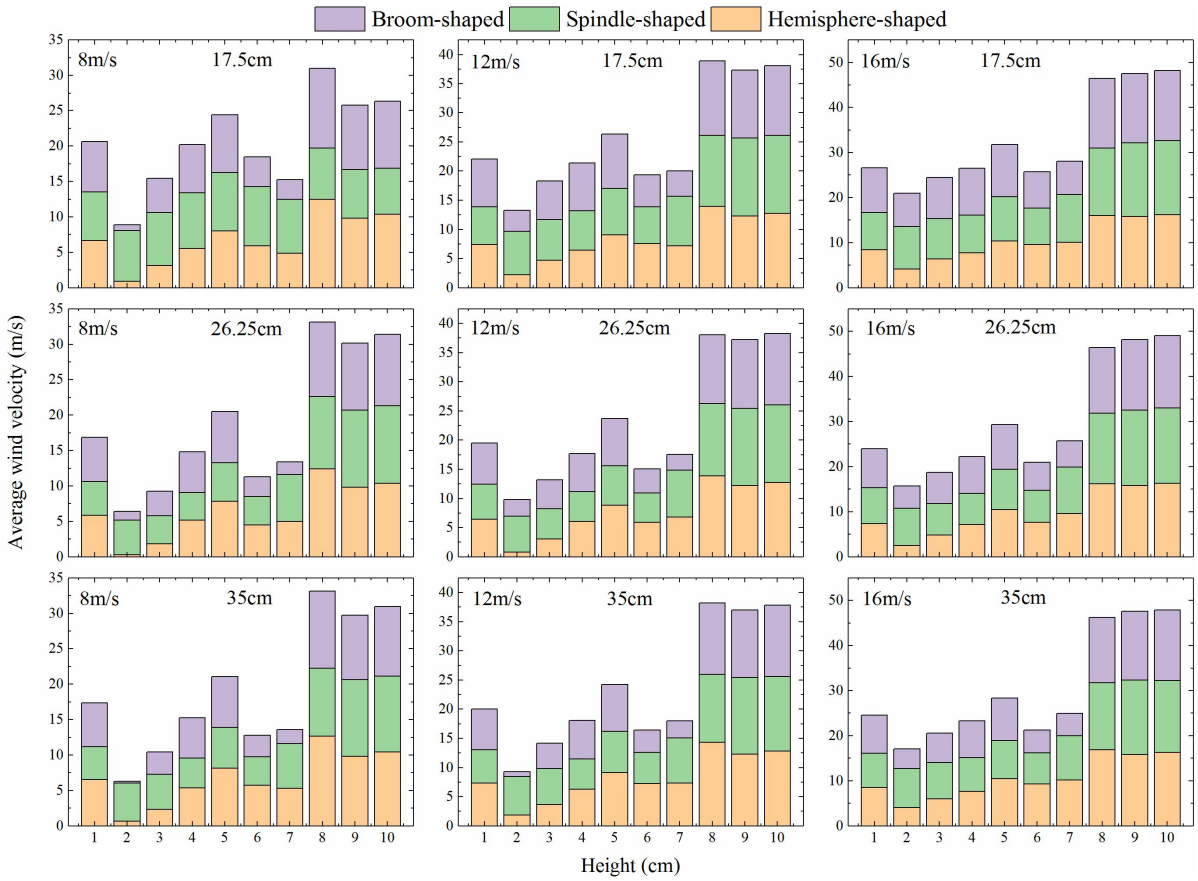

386 Figure 6 The average wind velocity of Pitot tubes in different heights of different spatial configurations with
387 simulated shrubs (hemisphere-shaped, spindle-shaped, and broom-shaped), row spaces (17.5 cm, 26.25 cm, and
388 35 cm), and net wind velocities (8 m/s, 12 m/s, and 16 m/s)

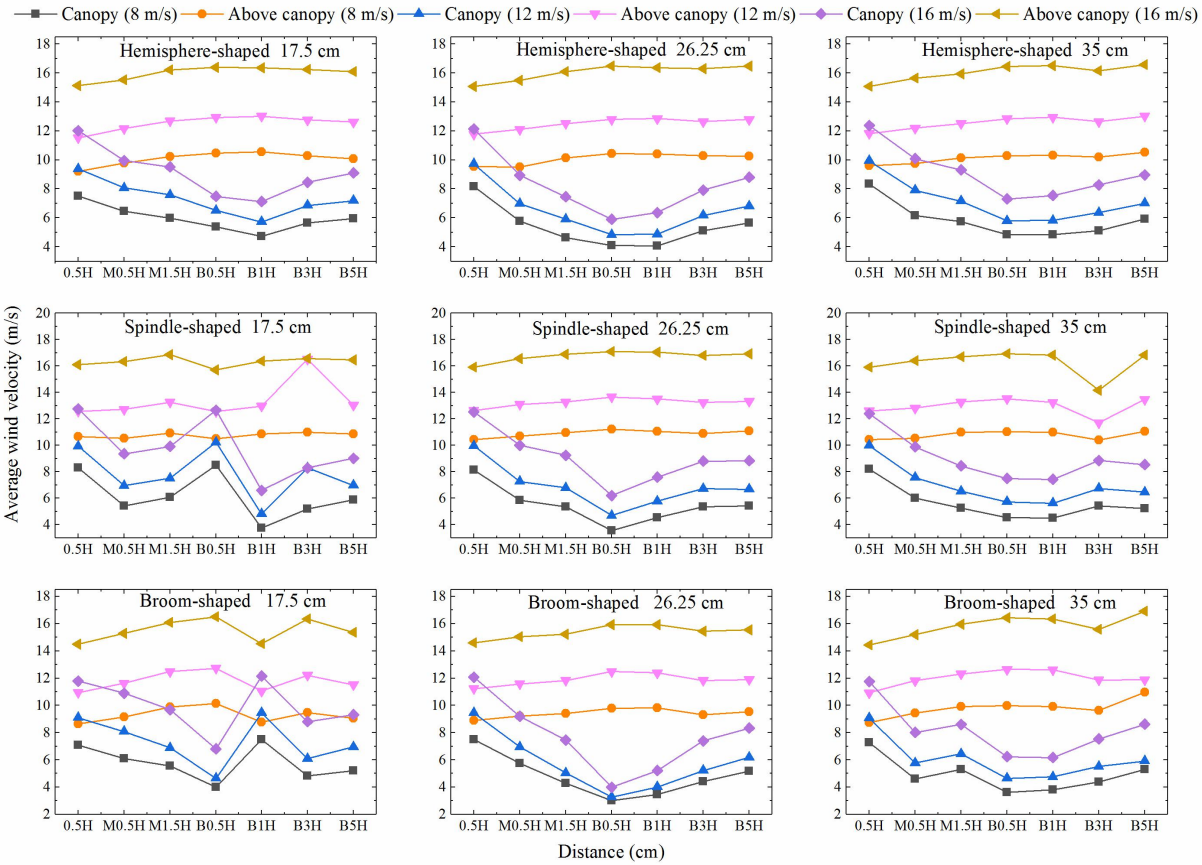

389 Figure 7 Profile of average wind velocity of different spatial configurations with simulated shrubs
390 (hemisphere-shaped, spindle-shaped, and broom-shaped), row spaces (17.5 cm, 26.25 cm, and 35 cm), and net
391 wind velocities (8 m/s, 12 m/s, and 16 m/s) (The wind velocity at the canopy is the average value of 0.2 cm, 0.5
392 cm, 1 cm, 2 cm, 4 cm, 8 cm, 12 cm, 16 cm, and the wind velocity above the canopy is the average value of 20
393 cm and 24 cm)

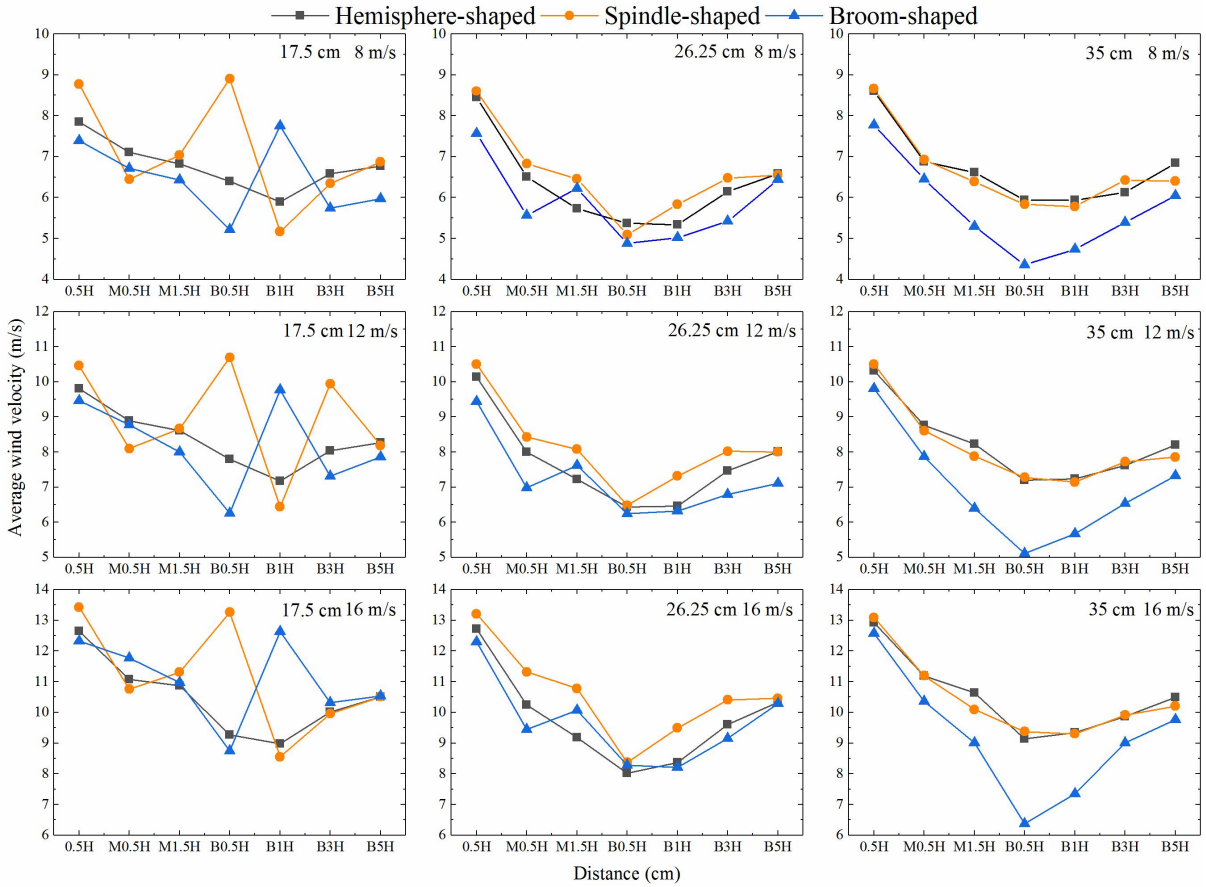

394 Figure 8 The average wind velocity of different spatial configurations with simulated shrubs
395 (hemisphere-shaped, spindle-shaped, and broom-shaped), row spaces (17.5 cm, 26.25 cm, and 35 cm), and net
396 wind velocities (8 m/s, 12 m/s, and 16 m/s)

397

398 Table 1 The characteristics parameters for field plants and wind tunnel models

Shrubs		Height (cm)	Canopy dimension (cm)	Canopy porosity (%)	Frontal area (m^2)
Field shrubs		89±11	70 (length) × 75 (width)	42–64	0.055–0.074
Synthetic shrubs	Hemisphere-shaped	22	15 (length) × 17.5 (width)	51	0.059
	Spindle-shaped	22	17.5 (length) × 15 (width)	47	0.052
	Broom-shaped	22	16 (length) × 16 (width)	55	0.062

399